Supporting Information

An Integrated Photoanode Based on Non-Critical Raw Materials for Robust Solar Water Splitting

Drialys Cardenas-Morcoso,[1] Miguel García Tecedor,[1] Tsvetelina Merdzhanova,[2] Vladimir Smirnov,[2] Friedhelm Finger,[2] Bernhard Kaiser,[3] Wolfram Jaegermann,[3] Sixto Gimenez[1*]

[1] Institute of Advanced Materials (INAM), Universitat Jaume I, Avenida de Vicent Sos Baynat, s/n, 12006 Castelló de la Plana, Castellón, Spain;

[2] IEK-5 Photovoltaik, Forschungszentrum Jülich, Jülich, 52425, Germany;

[3] Institute of Materials Science, TU Darmstadt, Darmstadt, 64287, Germany

Corresponding author: sjulia@uji.es

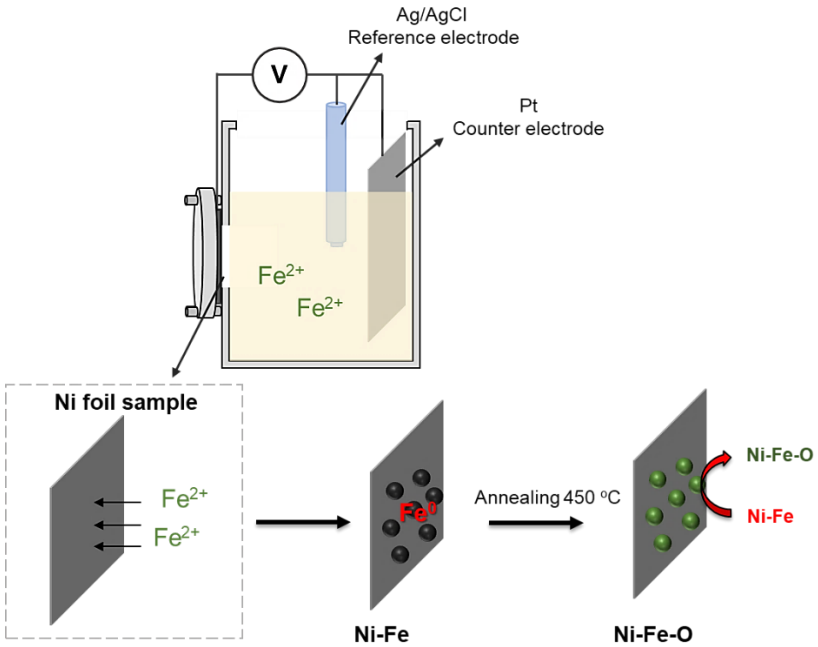

Figure SI1. Preparation of the Ni-Fe electrocatalyst by electrodeposition of metallic Fe on Ni foil, followed by thermal annealing to form the mixed Ni-Fe oxide.

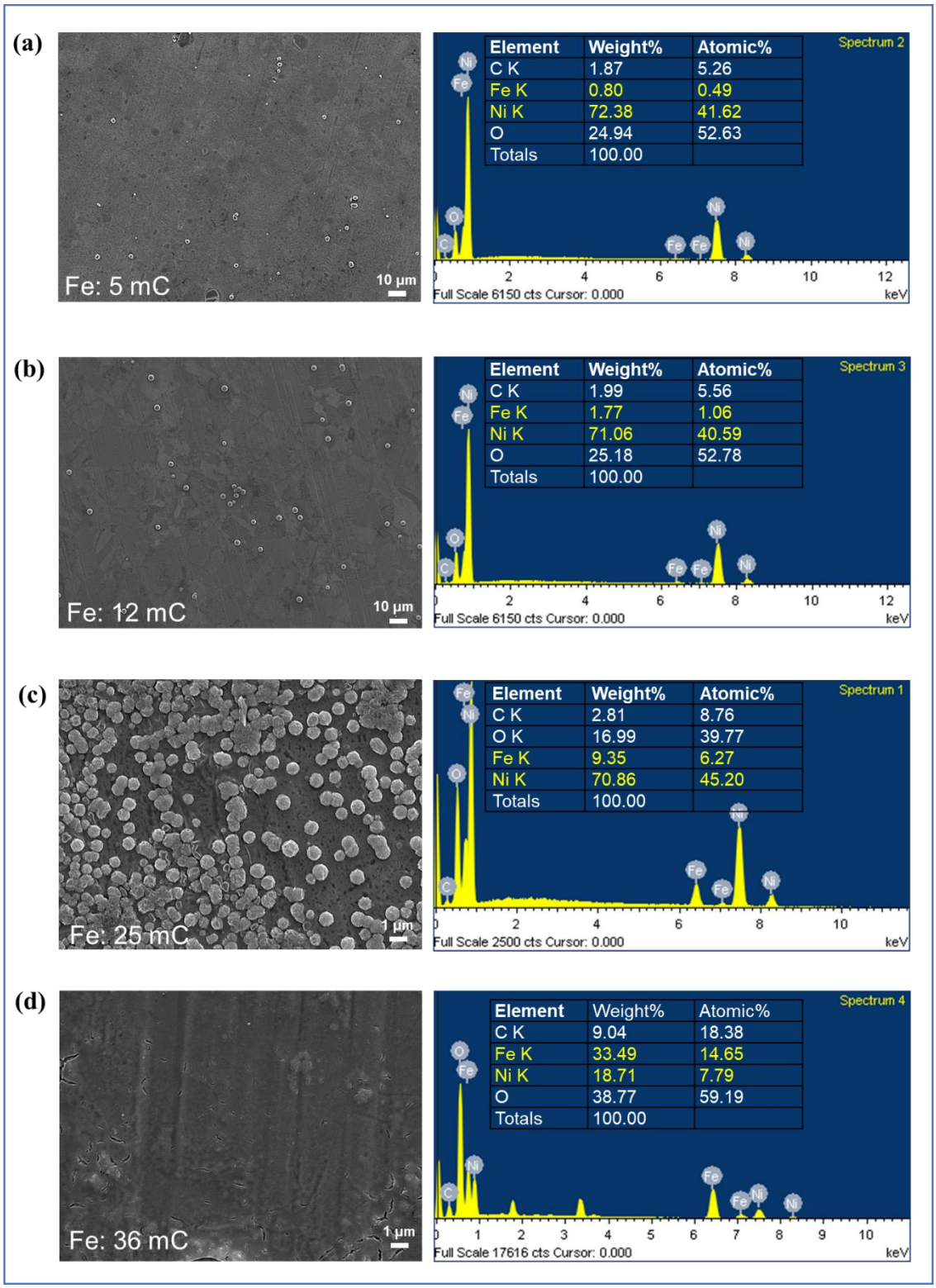

Figure SI2. SEM micrography and EDS analysis of thermally treated Ni substrate surfaces with **a.** 5 mC cm^{-2}, **b.** 12 mC cm^{-2}, **c.** 25 mC cm^{-2} **d.** 36 mC cm^{-2} Fe load.

Table SI1.- EDS analysis of the Ni films after different Fe electrodeposited charges.

	5 mC cm^{-2}	**12 mC cm^{-2}**	**25 mC cm^{-2}**	**36 mC cm^{-2}**
Element	**at.-%**	**at.-%**	**at.-%**	**at.-%**
C K	5.26	5.56	8.76	18.38
Fe K	**0.49**	**1.06**	**6.27**	**14.65**
Ni K	41.62	40.59	45.20	7.79
O	52.63	52.78	39.77	59.19

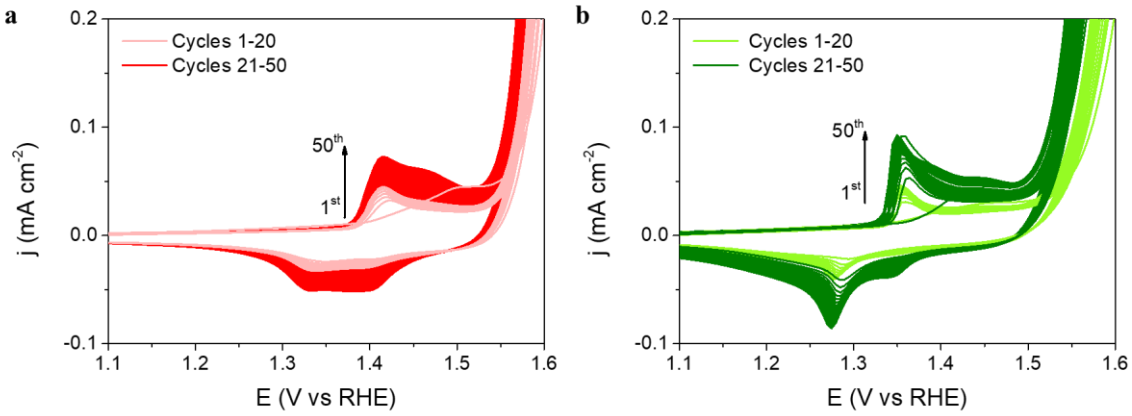

Figure SI3. Full cyclic voltammetry treatment performed on **a** bare Ni foil (thermally treated) and **b** Ni foil with 1.06 at-% Fe load.

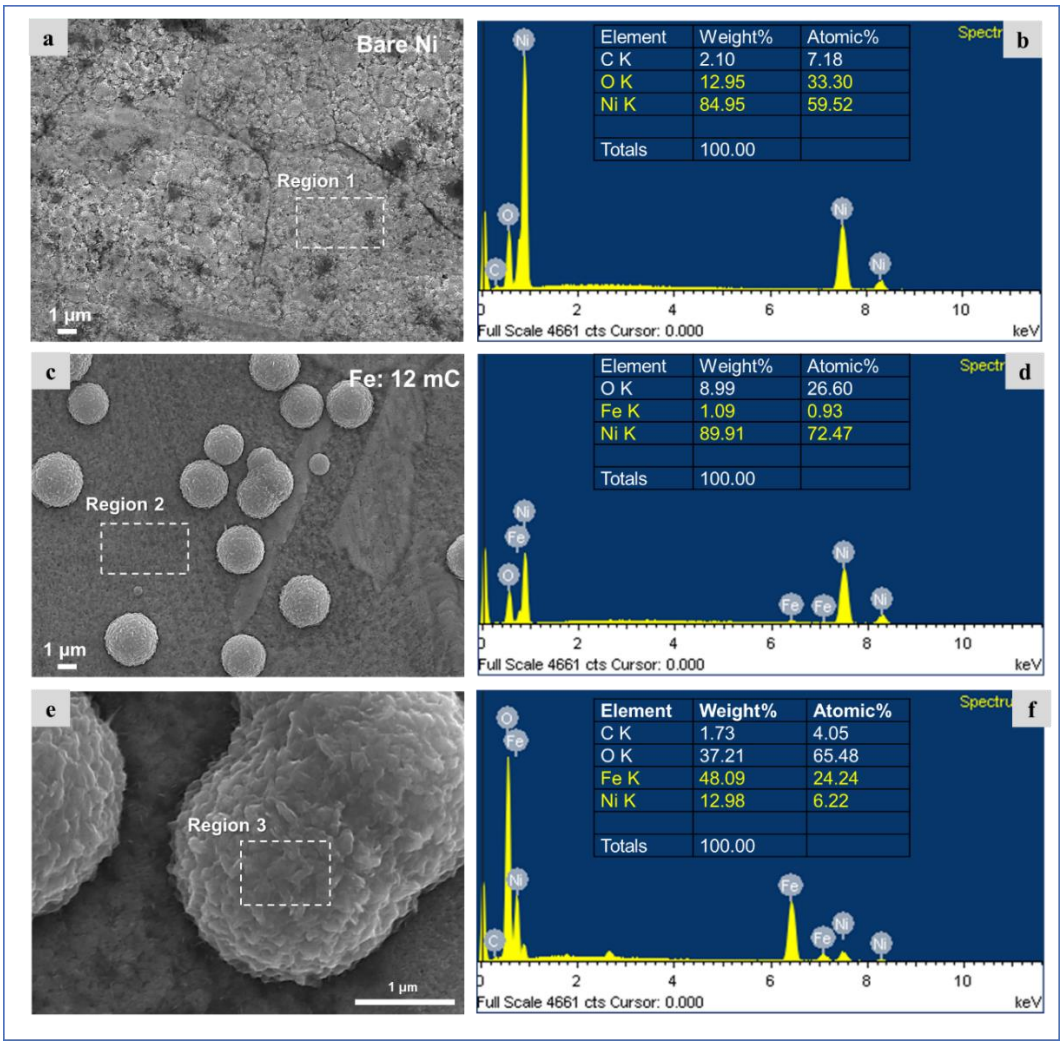

Figure SI4. SEM micrographs and EDS analyses of: **a** and **b:** reference Ni substrate after thermal annealing; **b, c, d** and **f:** two different regions of the Ni -Fe catalyst (1.06 at-% Fe).

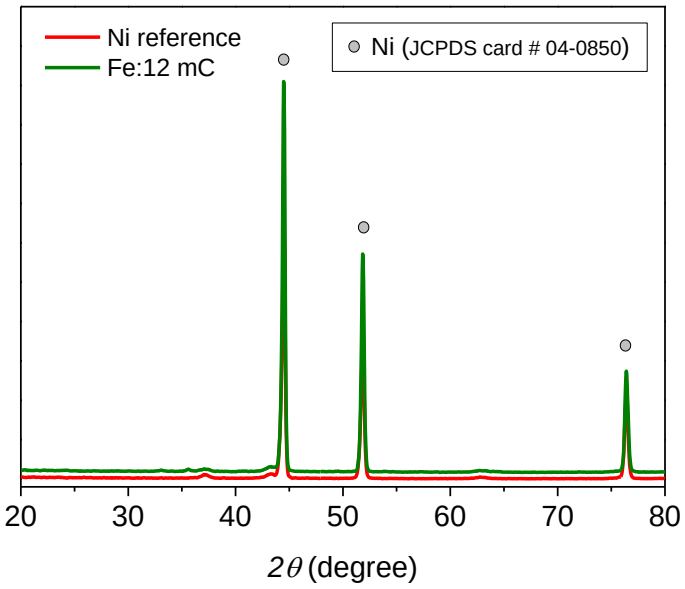

Figure SI5. XRD pattern of optimal Ni-Fe catalyst and reference Ni foil annealed.

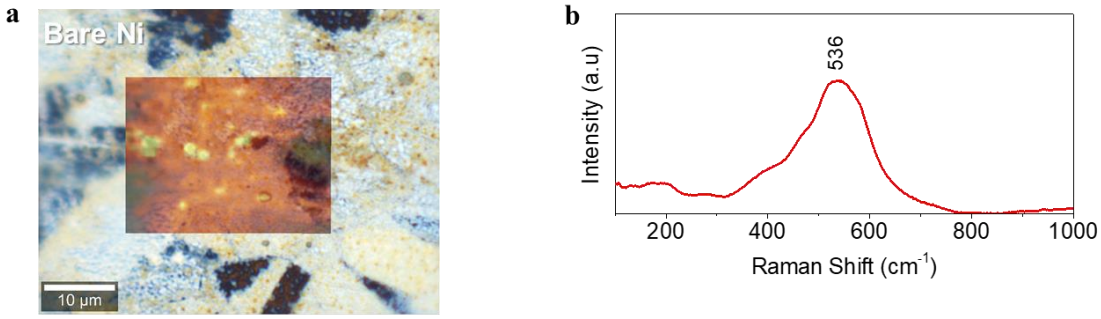

Figure SI6. Optical imagen of the Ni foil surface after annealing, taken as reference and Confocal Multi-Spectral Imaging (CMSI) maps in a selected area. **b.** Raman shift spectra corresponding to the selected area.

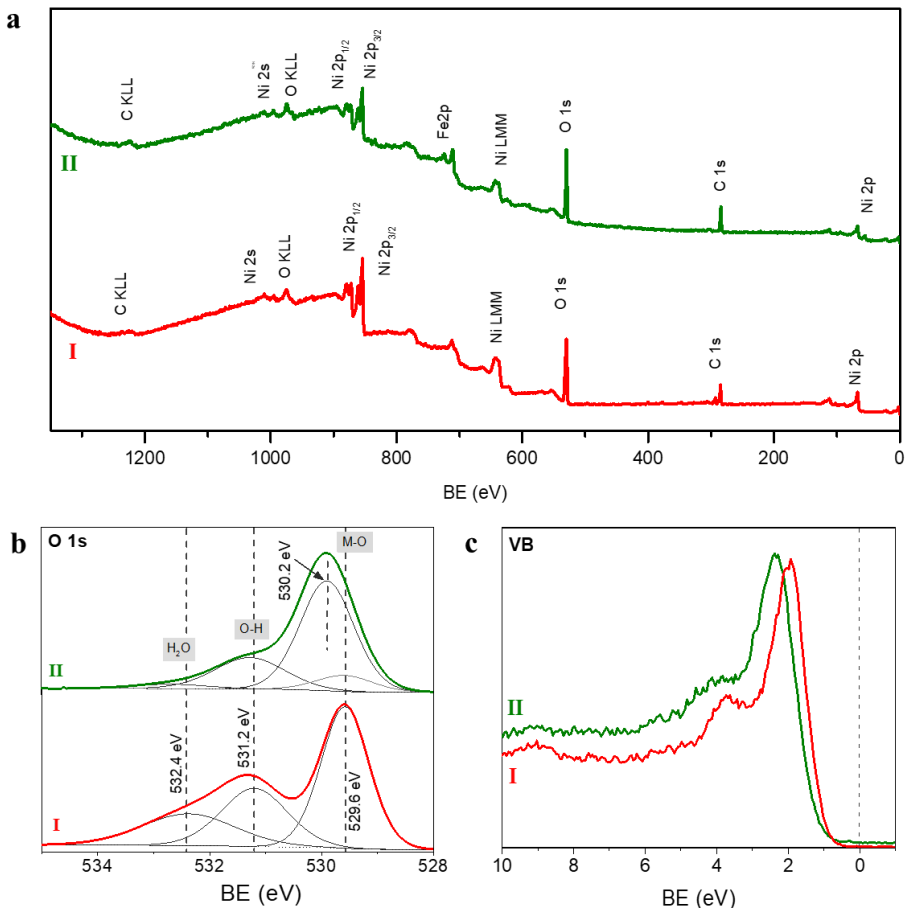

Figure SI7. XPS survey spectra of **I** bare, and **II** optimal Fe loaded Ni foil after annealing.

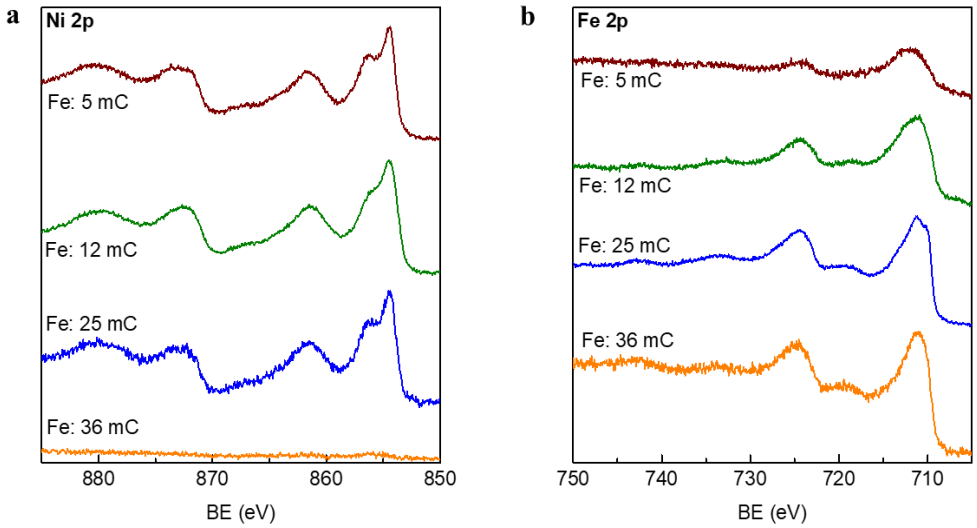

Figure SI8. a Ni 2p signal and **b** Fe 2p signal in XPS spectra of different samples prepared varying the Fe charge during the electrochemical deposition.

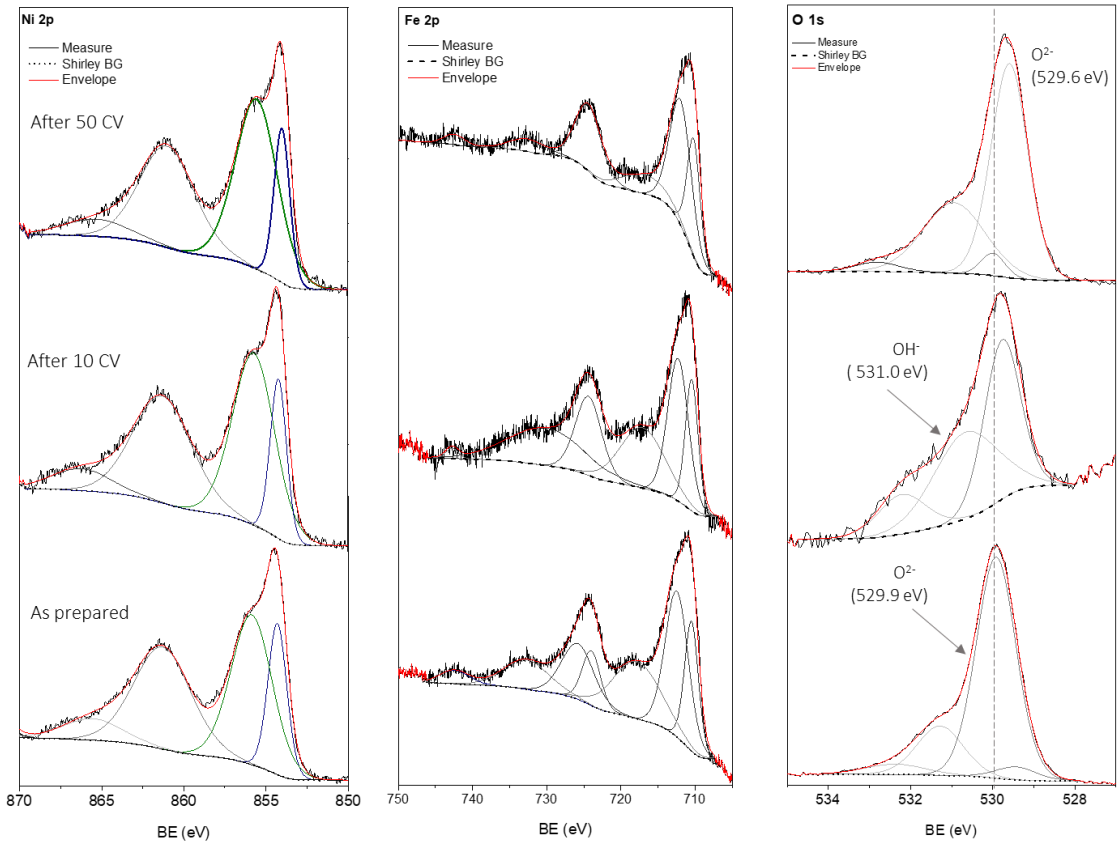

Figure SI9. XPS spectra at different stages of the electrochemical activation process for the optimal Ni-Fe electrocatalyst.

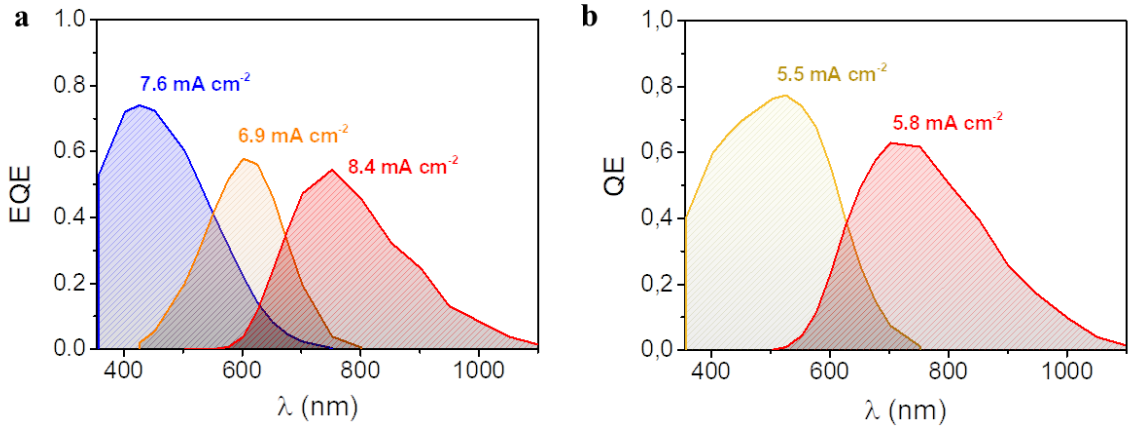

Figure SI10. Spectral response (external quantum efficiency, EQE), including individual spectra for each sub-cell, of the photovoltaic devices: **(a)** PV-1 **(b)** PV-2. The integrated current density value from the EQE spectrum for each sub-cell is placed in the respective measurement.

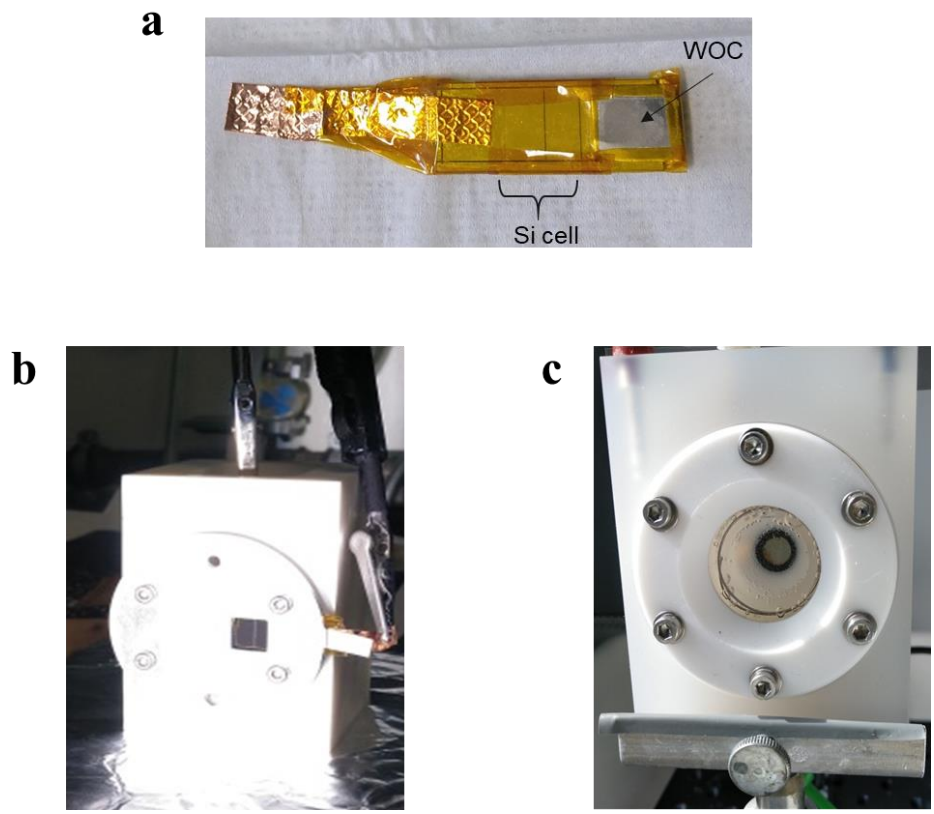

Figure SI11. a. Integrated PV-EC photoanode. The water oxidation electrocatalyst (WOC) is coupled to the Si multijunction PV device on the "p-side", whereas a Cu foil is used to transport the holes from the "n-side" to the counter electrode. The photoelectrochemical setup for characterization of the integrated device: **b.** View from the "back side" of the PV-EC device, showing the photoactive part, **c.** View from the "front side", showing the gas bubbles produced at the electrode surface.

Table SI2. Current density at the theoretical operation point and estimated STH efficiency.

	Ni reference		**Ni-Fe catalyst**	
Photovoltaic device	j_{op}	η_{STH}	j_{op} $(mA\ cm)^{-2}$	η_{STH}
PV-1	5.62	6.9%	6.09	7.5%
PV-2	5.28	6.5%	5.33	6.5%

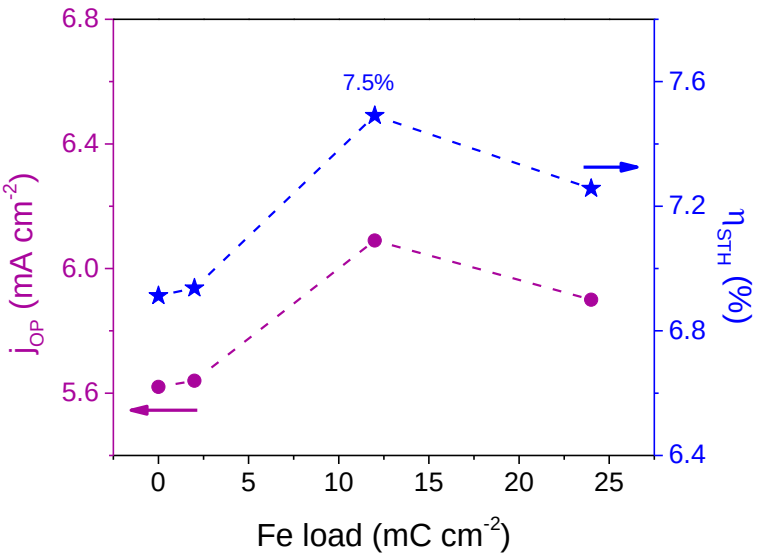

Figure SI12. Current density at the operation point (light blue circles) and STH efficiency (dark blue stars), as function of the Fe load on the electrocatalyst, in combination with the PV-1 device.

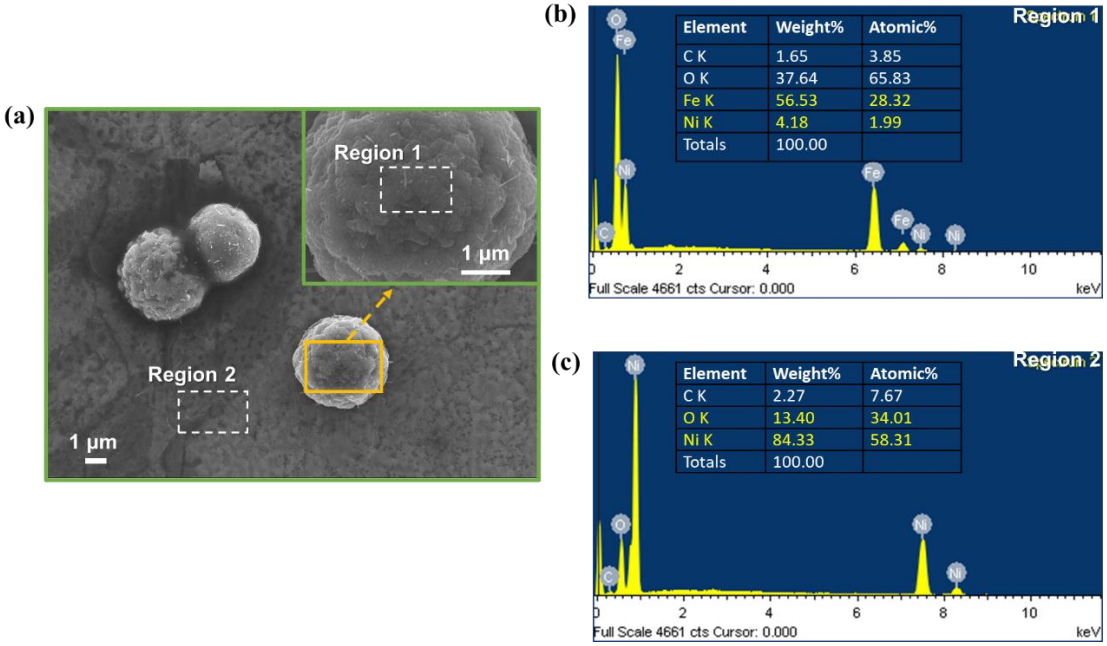

Figure SI13. Top view SEM micrograph and EDS analysis of the Ni-Fe electrocatalyst after the long-term (20 h) stability test.